REPORT DOCUMENTATION PAGE

Form Approved
OMB No. 0704-0188

1. REPORT DATE *(DD-MM-YYYY)*	2. REPORT TYPE	3. DATES COVERED *(From - To)*
05-02-2007	REPRINT	

4. TITLE AND SUBTITLE
The Study of State-Selected Ion-Molecule Reactions Using the Vacuum Ultraviolet Pulsed Field Ionization-Photoion Technique

5a. CONTRACT NUMBER

5b. GRANT NUMBER

5c. PROGRAM ELEMENT NUMBER
61102F

6. AUTHOR(S)
R.A. Dressler, Y. Chiu, D.J. Levandier*, X.N. Tang**, Y. Hou**, C. Chang**, C.Houchins**, H. Xu** and C. Ng**

5d. PROJECT NUMBER
2303

5e. TASK NUMBER
RS

5f. WORK UNIT NUMBER
A1

7. PERFORMING ORGANIZATION NAME(S) AND ADDRESS(ES)
Air Force Research Laboratory/VSBXT
29 Randolph Road
Hanscom AFB MA 01731-3010

8. PERFORMING ORGANIZATION REPORT NUMBER
AFRL-VS-HA-TR-2007-1010

9. SPONSORING / MONITORING AGENCY NAME(S) AND ADDRESS(ES)

10. SPONSOR/MONITOR'S ACRONYM(S)

11. SPONSOR/MONITOR'S REPORT NUMBER(S)

12. DISTRIBUTION / AVAILABILITY STATEMENT
Approved for Public Release; Distribution Unlimited

*Institute for Sci Research, Boston College, Chestnut Hill, MA,
**Dept of Chemistry, Univ of California, Davis, CA

13. SUPPLEMENTARY NOTES
REPRINTED FROM: The Journal of Chemical Physics, Vol 125, 132306 (2006)

14. ABSTRACT

This paper presents the methodology to generate beams of ions in single quantum states for bimolecular ion-molecule reaction dynamics studies using pulsed field ionization (PFI) of atoms or molecules in high-n Rydberg states produced by vacuum ultraviolet (VUV) synchrotron or laser photoexcitation. Employing the pseudocontinuum high-resolution VUV synchrotron radiation at the Advanced Light Source as the photoionization source, PFI photoions (PFI-PIs) in selected rovibrational states have been generated for ion-molecule reaction studies using a fast-ion gate to pass the PFI-PIs at a fixed delay with respect to the detection of the PFI photoelectrons (PFI-PEs). The fast ion gate provided by a novel interleaved comb wire gate lens is the key for achieving the optimal signal-to-noise ratio in state-selected ion-molecule collision studies using the VUV synchrotron based PFI-PE secondary ion coincidence (PFI-PESICO) method. The most recent development of the VUV laser PFI-PI scheme for state-selected ion-molecule collision studies is also described. Absolute integral cross sections for state-selected H_2^+ ions ranging from $v^+=0$ to 17 in collisions with Ar, Ne, and He at controlled translational energies have been obtained by employing the VUV synchrotron based PFI-PESICO scheme.

15. SUBJECT TERMS
Photoionization, State-selected chemical dynamics, Ion-molecule reactions, Pulsed-field Ionization, Rydberg molecules, Quasiclassical trajectories, Hydrogen molecular ion

16. SECURITY CLASSIFICATION OF:			17. LIMITATION OF ABSTRACT	18. NUMBER OF PAGES	19a. NAME OF RESPONSIBLE PERSON
a. REPORT	b. ABSTRACT	c. THIS PAGE			R. Dressler
UNCLAS	UNCLAS	UNCLAS	SAR		19b. TELEPHONE NUMBER *(include area code)* 781-377-2332

THE JOURNAL OF CHEMICAL PHYSICS **125**, 132306 (2006)

The study of state-selected ion-molecule reactions using the vacuum ultraviolet pulsed field ionization-photoion technique

Rainer A. Dressler[a] and Y. Chiu
Air Force Research Laboratory, Space Vehicles Directorate, Hanscom AFB, Massachusetts 01731-3010

D. J. Levandier
Institute for Scientific Research, Boston College, Newton, Massachusetts 02159

X. N. Tang, Y. Hou, C. Chang, C. Houchins, H. Xu, and Cheuk-Yiu Ng[b]
Department of Chemistry, University of California, Davis, California 95616

(Received 12 April 2006; accepted 1 May 2006; published online 4 October 2006)

This paper presents the methodology to generate beams of ions in single quantum states for bimolecular ion-molecule reaction dynamics studies using pulsed field ionization (PFI) of atoms or molecules in high-n Rydberg states produced by vacuum ultraviolet (VUV) synchrotron or laser photoexcitation. Employing the pseudocontinuum high-resolution VUV synchrotron radiation at the Advanced Light Source as the photoionization source, PFI photoions (PFI-PIs) in selected rovibrational states have been generated for ion-molecule reaction studies using a fast-ion gate to pass the PFI-PIs at a fixed delay with respect to the detection of the PFI photoelectrons (PFI-PEs). The fast ion gate provided by a novel interleaved comb wire gate lens is the key for achieving the optimal signal-to-noise ratio in state-selected ion-molecule collision studies using the VUV synchrotron based PFI-PE secondary ion coincidence (PFI-PESICO) method. The most recent development of the VUV laser PFI-PI scheme for state-selected ion-molecule collision studies is also described. Absolute integral cross sections for state-selected H_2^+ ions ranging from $v^+=0$ to 17 in collisions with Ar, Ne, and He at controlled translational energies have been obtained by employing the VUV synchrotron based PFI-PESICO scheme. The comparison between PFI-PESICO cross sections for the $H_2^+(HD^+)+Ne$ and $H_2^+(HD^+)+He$ proton-transfer reactions and theoretical cross sections based on quasiclassical trajectory (QCT) calculations and three-dimensional quantum scattering calculations performed on the most recently available *ab initio* potential energy surfaces is highlighted. In both reaction systems, quantum scattering resonances enhance the integral cross sections significantly above QCT predictions at low translational and vibrational energies. At higher energies, the agreement between experiment and quasiclassical theory is very good. The profile and magnitude of the kinetic energy dependence of the absolute integral cross sections for the $H_2^+(v^+=0-2,N^+=1)+He$ proton-transfer reaction unambiguously show that the inclusion of Coriolis coupling is important in quantum dynamics scattering calculations of ion-molecule collisions. © *2006 American Institute of Physics*. [DOI: 10.1063/1.2207609]

I. INTRODUCTION

The understanding of state-selected and state-to-state unimolecular and bimolecular reaction dynamics is of fundamental importance in the quest to control the outcome of chemical reactions. Research on gas-phase ion-molecule reactions has made critical contributions to the understanding of state-selected reaction dynamics.[1,2] This is primarily related to several experimental advantages that the study of ion-molecule reactions offers compared to the study of neutral-neutral reactions. The most significant advantage is that reactant ions in a wide range of internal states, including metastable states, can be prepared by photoionization of appropriate precursor neutral molecules. Employing various photoionization techniques, ion-molecule reaction experiments have been remarkably successful in studying the internal energy dependence of ion-molecule reaction dynamics,[3–11] including vibrational-mode reactivity of polyatomic ions[12–14] and spin-orbit-state effect of atomic ions.[1,2] The ability for reactant ion state preparations, together with the fact that ions can readily be electrostatically accelerated and efficiently detected by using mass filters and trapping and guiding devices, has allowed accurate absolute state-selected cross section measurements for many ion-molecule processes over wide kinetic energy ranges. The translational energy dependence of state-selected ion-molecule reaction cross sections provides the ultimate test of potential energy surfaces and thus invaluable insight into the ion-neutral collisions dynamics, in particular, to nonadiabatic processes such as charge-transfer reactions.[1,15,16]

Apart from the motivation for a fundamental understanding of molecular reaction dynamics, an important incentive for determining absolute state-selected cross sections of ion-

[a]Electronic mail: rainer.dressler@hanscom.af.mil
[b]Electronic mail: cyng@chem.ucdavis.edu

neutral processes is their importance in models of atmospheric, industrial, and aerospace plasmas.[17–21] It is known that atomic and diatomic ions initially produced by solar UV photoionization of atmospheric gases have nonequilibrium internal energy distributions that affect the atmospheric dynamics and phenomenology.[17,18] Thus, quantitative state-selected laboratory measurements of rate constants and cross sections of relevant atmospheric ions are required for modeling of chemical reaction cycles in planetary atmospheres.

The progress in state-selected ion-molecule reaction experiments has depended on the development of photoionization techniques.[22–27] The pioneering work of Chupka *et al.*[22–24] has demonstrated that single-photon vacuum ultraviolet (VUV) photoionization is a general and versatile method for the preparation of state- or energy-selected reactant ions. Due to the fine control in photon energy, reactant ions in their ground states can be easily prepared with 100% purity by photoionization at the ionization or dissociative ionization threshold of appropriate precursor molecules.[2,22–25] In principle, reactant ions of known, but different distributions of internal states can be produced by tunable VUV photoionization. Mediation of near resonance autoionization states can aid in preparing reactant ion vibrational states with negligible Franck-Condon factors when photoionizing with a tunable VUV source.[28] Chupka *et al.* have shown that the autoionization mechanism for H_2 allows the preparation of $H_2^+(v^+=0-4)$ with high purity.[22–24] Using a VUV photoionization mass spectrometer, they examined the reactivities of state-selected $H_2^+(v^+=0-4)$ with rare gases in the ion source. However, since reactions occurred as the reactant ions were extracted out of the ion source, the collision energies of the experiment were ill defined. The derived reaction cross sections must, therefore, be considered to be phenomenological cross sections and comparison thereof to theoretical cross sections is tenuous. Lee and co-workers[7,8] are the first to combine the VUV photoionization mass spectrometric method with the radio-frequency ion guide technique[29,30] for absolute state-selected cross section measurements of a series of reactions involving H_2^+, D_2^+, and HD^+. Ng and co-workers further extended these methods and, with the inclusion of the differential reactivity technique, obtained absolute state-to-state cross sections for the $Ar^+(^2P_{3/2,1/2})+Ar$, H_2, and $H_2^+(v^+)+Ar$ reactions.[2,25,31–33]

Pulsed laser based resonance-enhanced multiphoton ionization (REMPI) methods have also been successfully used to prepare state-selected reactant ions for ion-molecule reaction cross section measurements.[12–14,26] The REMPI approach involves excitation of the precursor neutral molecule to a Rydberg state with vibrational character given by the ion core. The photoionization of the excited Rydberg molecule in a selected vibrational state by the absorption of an additional laser photon then produces the ion in the corresponding vibrational state with high purity. Although the REMPI photoelectron spectrum can provide information on the vibrational state distribution of the nascent REMPI ion, the initial internal state distribution of the ion could be altered by the absorption of an additional laser photon.

When a continuous or pseudocontinuous VUV light source is used, the most versatile method for state-selected reactant ion preparation is the photoelectron-photoion coincidence technique, which takes advantage of the time correlation of the photoelectron-photoion pair produced from the same precursor neutral species.[1,4–6,9,10,27] By virtue of the high detection sensitivity and energy resolution, the VUV threshold photoelectron-photoion coincidence (TPEPICO) time-of-flight (TOF) scheme has been the method of choice and has been successfully used for unimolecular reaction dynamics studies of state- or energy-selected ions.[34] The extension of this technique for bimolecular state-selected ion-molecule reaction studies, referred to in the literature as the threshold photoelectron (TPE)-secondary ion coincidence (TPESICO) method, has also been very successful.[1,4–6,27] Due to the dispersion of the product ion arrival times, the coincidence TOF peaks for product ions are significantly broader than those observed in unimolecular studies. It has been shown that the signal-to-noise ratio for a biomolecular experiment can be 100-fold lower than that for a unimolecular study.[35,36] As a result of the limited signal-to-noise ratio and energy resolutions, TPESICO experiments have been restricted to a relatively narrow range of internal energy levels of the reactant ion in comparison to the reactant ion dissociation energy.

The pulsed field ionization-photoelectron (PFI-PE) scheme[37–43] is a variant of the TPE method, which is based on the detection of zero kinetic energy electrons. Since the PFI-PE scheme is free from the electron hot-tail problem that afflicts the TPE method, it has been shown to achieve significantly higher energy resolution. The recent development of a broadly tunable, high-resolution VUV undulator synchrotron radiation source,[44] along with the pulsed field ionization-photoelectron-photoion[45] (PFI-PEPICO) and PFI-PE-secondary ion coincidence (PFI-PESICO) methods[46,47] at the Chemical Dynamics Beamline of the Advanced Light Source (ALS), has substantially increased the detection sensitivity and the range of internal state selectivity for unimolecular and bimolecular reaction studies of state-selected ions. In particular, the high sensitivity and high energy resolution nature of the PFI-PESICO method has resulted in measurements of reaction cross sections of reactant ions excited to vibrational energy levels within less than 0.1 eV of the dissociation limit of the reactant ions.[47,48]

The present paper is a summary of the results obtained using the synchrotron based PFI-PESICO technique. The present article is structured as follows. In Sec. II, the salient features of the PFI-PESICO technique using multibunch synchrotron radiation of the ALS is introduced. We then discuss the $H_2^+(v^+)$ and $HD^+(v^+)$ proton transfer reactions with rare gas atoms, to which the technique was first applied.[48,49] These highly fundamental reaction systems are particularly attractive because they have been the subject of extensive theoretical work including the development of accurate three-dimensional (3D) *ab initio* potential energy surfaces for the He and Ne systems.[50–52] As will be demonstrated, the present results pose new challenges to theorists as they raise the total collision energy of reaction systems with an ever increasing number of accessible states. We close the paper with a discussion of what lies ahead in this exciting field of

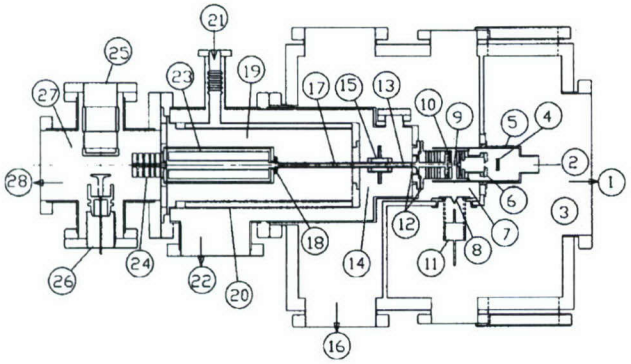

FIG. 1. Schematic diagram for the octopole-quadrupole photoionization apparatus. (1) To 2000 L/s turbomolecular pump, (2) to 300 L/s turbomolecular pump, (3) molecular beam source chamber, (4) dual MCP photoelectron detector, (5) μ-metal shield, (6) electron TOF spectrometer, (7) photoionization chamber, (8) skimmer, (9) photoionization center, (10) wired ion gate lens, (11) nozzle and nozzle holder, (12) ion injection lenses, (13) short rf octopole (8.6 cm), (14) reaction chamber, (15) reaction gas cell, (16) to 800 L/s turbomolecular pump, (17) long rf octopole (19.6 cm), (18) entrance ion lenses for QMS, (19) QMS chamber, (20) liquid nitrogen cooled wall, (21) liquid nitrogen inlet, (22) to 800 L/s turbomolecular pump, (23) QMS, (24) exit ion lenses for QMS, (25)+(26) Daly ion detector, (27) detector chamber, and (28) to 600 L/s turbomolecular pump. Taken from Ref. 46.

research, including the development of the VUV laser based PFI-photoion (PFI-PI) or mass analyzed threshold ion technique[39] for the preparation of rovibronic state-selected reactant ions for ion-molecule collision studies.

II. EXPERIMENTAL CONSIDERATIONS

The octopole-quadrupole photoionization apparatus at the ALS and its application for PFI-PEPICO (Refs. 38 and 45) and PFI-PESICO (Refs. 46–49) measurements have been described in detail previously. Briefly, this apparatus (Fig. 1) consists of, in sequential order, a PFI-PEPICO ion source for the internal state selection of reactant ions, an interleaved comb wire ion gate lens (10) for the rejection of false coincidence ions, an ion-molecule collision region with reaction gas cell and dual rf octopole ion guide [(13)+(15)+(17)] for efficient collection of product ions, a quadrupole mass spectrometer (QMS) (23) for reactant and product ion mass discrimination, and a Daly scintillation detector [(25)+(26)] for ion detection. The octopole-quadrupole photoionization apparatus is partitioned into four differentially pumped chambers, namely, the molecular beam source chamber (3), the photoionization chamber (7), the reaction chamber (14), and the quadrupole chamber (19), which are evacuated by separate turbomolecular pumps. The dual rf octopole ion guide consists of a short (13) and a long (17) octopole unit, which are powered by a single rf power supply. The reaction gas cell (15) encompasses the last part of the short rf octopole. Because different dc potentials can be applied to the long and short octopoles, slow primary product ions, such as charge transfer product ions, can be extracted from the reaction cell to minimize secondary reactions. In addition to integral cross sections, the experimental setup is capable of measuring differential cross sections through a secondary ion TOF analysis.[30]

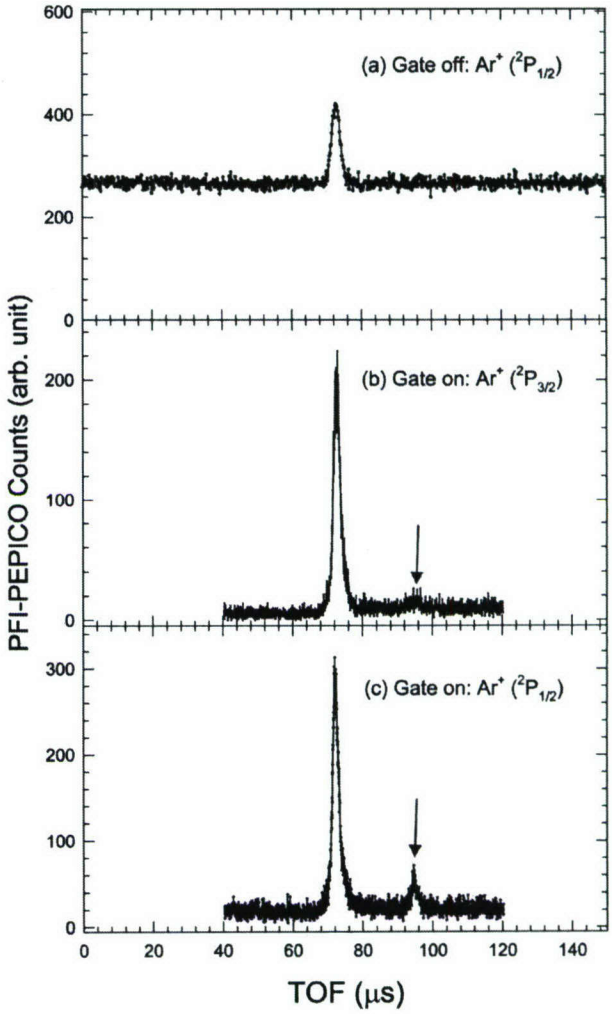

FIG. 2. TOF spectra of PFI-PEPICO ions demonstrating the effectiveness of the interleaved comb fast ion gate. (a) The gate is set to continuously transmit $Ar^+(^2P_{1/2})$ ions. (b) Double gate operation to transmit $Ar^+(^2P_{3/2})$ ions. (c) Double gate operation to transmit $Ar^+(^2P_{1/2})$ ions. The arrows point to arrival time of false coincidence ions transmitted during second gate opening. Taken from Ref. 46.

The signal-to-noise ratio of the PFI-PESICO experiment was dramatically improved with the novel application of the fast ion gate (10).[46] The interleaved comb[53,54] produces a highly local, strong perpendicular electric field that can be rapidly turned off to pass the state-selected PFI-PI at a fixed delay with respect to the detection of a PFI-PE, while rejecting background false coincidence ions arriving at a time different from the PFI-PIs when the gate field is turned on. The signal-to-noise ratio improvement attributable to the fast ion gate is demonstrated in Fig. 2, where we compare PFI-PEPICO TOF spectra for $Ar^+(^2P_{3/2,1/2})$ observed with and without operation of the fast ion gate.[46] Figure 2(a) shows the PFI-PEPICO TOF spectrum for $Ar^+(^2P_{1/2})$ formed by photoionization of an effusive Ar beam at 298 K when the ion gate transmits all ions. The intensity of background false coincidences in the spectrum of Fig. 2(a) is a factor of ~2 higher than the coincidence peak. Figures 2(b) and 2(c) depict the PFI-PEPICO TOF spectra for $Ar^+(^2P_{3/2})$ and

$Ar^+(^2P_{1/2})$, respectively, with the ion gate in operation. The ion gate (duration=200 ns) was opened twice for each PFI-PE trigger pulse. The first ion gate was opened at the correct delay of 4.7 μs with respect to the PFI-PE trigger pulse to pass the true PFI-PIs, whereas the second ion gate was opened after an arbitrary delay of 25 μs with respect to the first ion gate. Thus, the first TOF peak measures mostly the intensity of true coincidence ions, whereas the second TOF peak [marked by arrows in Figs. 2(b) and 2(c)] provides a measure of false coincidence ion count rates at the given gate width. The true coincidence counts can thus be obtained by taking the difference in counts of the first and second TOF peaks. As shown in Fig. 2(c), the background false coincidences were reduced to $\approx$14% of the true coincidence $Ar^+(^2P_{1/2})$ PFI-PIs by using the differential ion gate[55,56] PFI-PEPICO scheme.

With this approach, absolute reaction cross sections for state-selected ion-molecule reactions have been determined for the ion-molecule reactions of $H_2^+(v^+=0-17,N^+)$ with He, Ne, and Ar.[46–49] The rotationally resolved vibrational PFI-PE bands for $H_2^+(v^+=0-18)$ have been obtained previously.[2,57] Due to the rotational distributions of *ortho* and *para* hydrogen at 298 K and selection rules for photoionization, the $N^+=0$, 1, 2, and 3 rotational states for many vibrational v^+ states for H_2^+ can be prepared with good intensities by photoionization of normal H_2 at 298 K.[57,58]

Application of the PFI-PESICO method is demonstrated in Fig. 3 for the $H_2^+(v^+=2,N^+=0)+Ar$ reaction system that produces Ar^+ and ArH^+ ions.[46] Figure 3(a) shows the PFI-PEPICO TOF spectrum for reactant $H_2^+(v^+=2,N^+=0)$ recorded at the laboratory ion energy of 2.5 eV using the differential fast-ion-gate scheme. The first ion gate (duration =300 ns) is delayed by 1.50 μs with respect to the PFI-PE detection and the second ion gate (duration=300 ns; we note that the actual arrival time interval of H_2^+ at the ion gate is less than 200 ns) is set at 150 μs with respect to the first ion gate. The PFI-PEPICO spectrum of Fig. 3(a) only reveals a strong TOF peak at 13 μs, and a second TOF peak at $\approx$163 μs, which would represent the false coincidences, is not discernible. This observation indicates that the TOF peak at 13 μs is entirely due to true coincidences.

The spectra shown in Figs. 3(b) and 3(c) are the PFI-PESICO TOF spectra of product Ar^+ and ArH^+, respectively, obtained for an accumulation time of 50 min by using an Ar gas cell pressure of 2.15×10^{-4} Torr.[46] Figures 3(b) and 3(c) indicate that the arrival times for product ArH^+ ions are in the range of $\approx$100–200 μs, which is shorter than that of $\approx$100–250 μs for charge transfer Ar^+ where momentum transfer is negligible. The intensities for reactant H_2^+ $(v^+=2,N^+=0)$ and product Ar^+ and ArH^+ ions are measured by their respective coincidence counts after normalizing with the respective number of PFI-PE triggers. The absolute integral reaction cross sections for Ar^+ and ArH^+ can then be calculated by the ratio of the product and reactant ion intensities, the neutral reactant gas density, and the calibrated effective length of the gas cell.[46]

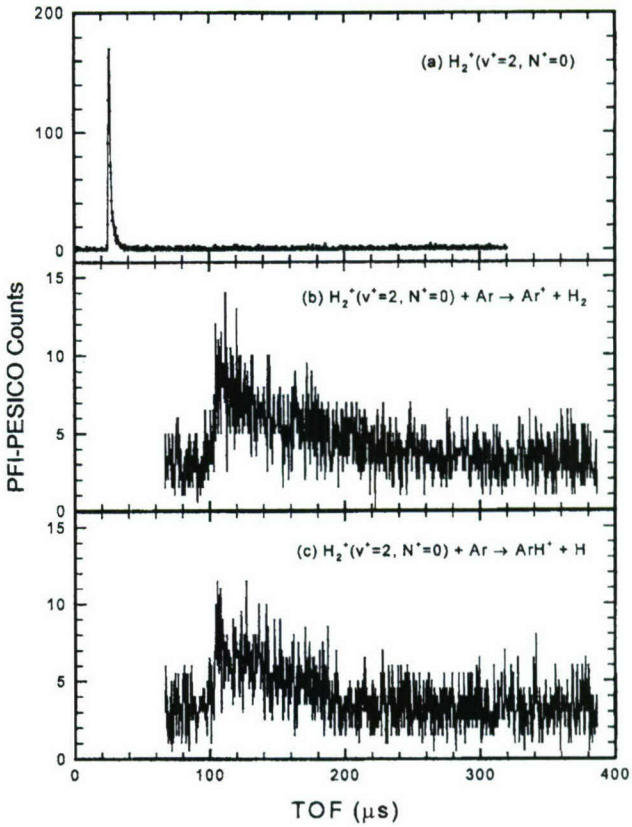

FIG. 3. TOF spectra of PFI-PESICO ions observed in $H_2^+(v^+=2,N^+=0)$ +Ar collisions. (a) Primary ion PFI-PEPICO spectrum. (b) Ar^+ product ion PFI-PESICO spectrum. (c) ArH^+ product ion PFI-PESICO spectrum. Taken from Ref. 46.

III. RESULTS AND DISCUSSION

A. The $H_2^+(X,v^+,N^+=1)+Ar$ collision system

The $H_2^+(v^+)+Ar$ reaction system

$$H_2^+ + Ar \rightarrow H_2 + Ar^+ \quad \Delta H = 0.33 \text{ eV} \tag{1}$$

$$\rightarrow H + ArH^+ \quad \Delta H = -1.15 \text{ eV} \tag{2}$$

has been previously examined in detail for the lowest reactant vibrational levels $v^+=0-4$.[25,27,32] Given the relatively large cross sections, it was a logical choice for a first test of the PFI-PESICO method. We have determined the PFI-PESICO cross sections for the sum of product Ar^+ and ArH^+ with relative ease for vibrational levels $v^+=0-17$, as shown in Fig. 4. The error bars are the statistical errors. It is seen that even for $v^+=17$, which is the second to the last bound vibrational level of H_2^+ and lies a mere 0.03 eV below the dissociation limit, an accurate measurement could be performed. The observed cross sections for low v^+ levels agree well with the previous measurements.[25,27] A relatively sharp maximum is observed for $v^+=2$, which can be attributed to a charge-transfer resonance. At the higher v^+ levels, the cross sections are observed to be relatively independent of reactant vibrational energy until above $v^+=14$, where a slight drop is observed. That may be attributable to competition with the collision-induced dissociation (CID) channel:

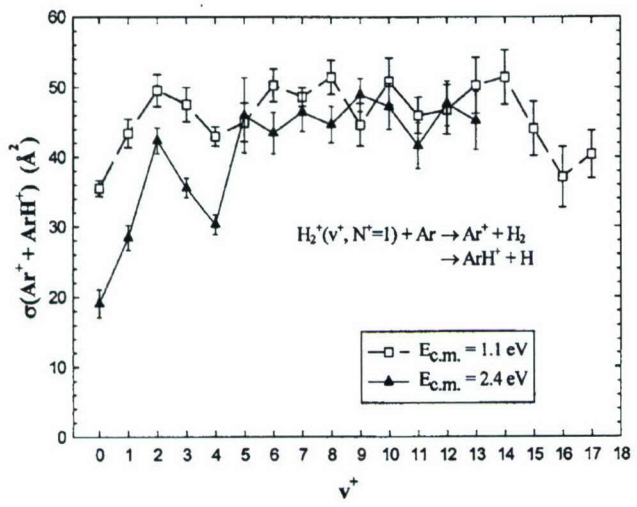

FIG. 4. Absolute total cross sections for Ar^+ and ArH^+ [$\sigma_{v^+}(Ar^+ + ArH^+)$] formed in the $H_2^+(X, v^+, N^+=1)+Ar$ reaction at $E_{c.m.}=1.1$ (□) and 2.4 eV (▲) in the v^+ range of 0–17. Taken from Ref. 47.

$$H_2^+ + Ar \rightarrow H^+ + H + Ar, \quad \Delta H = 2.65 \text{ eV} \tag{3}$$

which is open for $v^+=7$ and 1 at translational energies of 1.1 and 2.4 eV, respectively.[47] It is somewhat surprising that effects due to dissociation are not noticed at lower reactant vibrational levels. However, measurements of the CID cross sections for $v^+=0-4$ show that they are below 1 Å^2 at 2.4 eV and thus do not compete with the more efficient proton transfer and charge-transfer channels.[32] The survival of proton-transfer products for barely bound reactant molecular ions is consistent with a spectator stripping mechanism in which the product H atom is an unaffected "spectator" of the reactive collision.[59,60] Although the branching ratio for proton transfer to charge transfer was not determined for $v^+=17$, similar weak competition of the CID channel was observed for the "pure" proton-transfer system, H_2^++Ne,[48] discussed subsequently. In case of the charge-transfer channel, the relative independence of the cross section as a function of vibrational quantum number at high v^+ can be rationalized by the increased number of near-resonant $v^+ - v$ transitions with significant Franck-Condon factors.

Reliable theoretical results at the vibrational energies of the present experiment are not expected in the near future, given the complexity of this reaction system involving multiple potential energy surfaces and significant spin-orbit coupling. The most recent work on the $(Ar+H_2)^+$ collision system has still been limited to using a diatomics in molecule (DIM) approach with limited long-range accuracy.[61,62] The H_2^++Ne and He proton-transfer systems, on the other hand, have been the subject of copious theoretical studies since they can be treated as proceeding on a single potential energy surface at low collision energies.

B. The H_2^+, $HD^+(X, v^+)$+Ne proton-transfer system

The $H_2^+(v^+)$+Ne charge-transfer reaction is highly endothermic. The charge-transfer surface, consequently, will not be an important factor in the dynamics of this collision system at hyperthermal collision energies comparable to the H_2^+ binding energy. The endothermic proton-transfer reaction

$$H_2^+ + Ne \rightarrow H + NeH^+, \quad \Delta H = 0.54 \text{ eV}, \tag{4}$$

has long been regarded as a textbook example of vibrational enhancement of chemical reactions. Reaction (4) was the subject of the earliest state-selected ion-molecule reaction studies of Chupka and Russell,[24] who used monochromatic VUV radiation to selectively populate reactant ions in vibrational levels $v^+=0-7$ via autoionization resonances. The derived phenomenological cross section measurements were followed by thermal energy coincidence studies by Pijkeren *et al.*[9,10] that determined relative proton-transfer rate coefficients from threshold up to $v^+=8$. TPESICO measurements of relative proton-transfer cross sections by Herman and Koyano[63] for $v^+=0-4$ at translational energies ranging from 0.46 to 3.5 eV demonstrated that vibrational energy was significantly more effective than translational energy in promoting the reaction.

These exciting experimental advances spurned a significant body of theoretical work.[52,64–72] Theoretical studies on 3D potential energy surfaces exhibited stark differences between quasiclassical trajectory (QCT) and quantum scattering calculations of integral cross sections. The discrepancy was attributed to long-lived resonances appearing as structure in the cross section energy dependence determined in the quantum scattering studies.[68–72] Except for the phenomenological cross sections by Chupka *et al.*,[22–24] and unpublished measurements by Gerlich and co-workers that appeared in the theoretical work of Urban *et al.*,[68] the theorists had limited absolute integral cross section data to compare their results to. For this reason, the PFI-PESICO guided-ion beam apparatus was used to measure the collision energy (center of mass) dependence of the H_2^++Ne proton-transfer integral cross section for the two lowest reactant vibrational levels at high signal-to-noise ratio through ion preparation using intense autoionization resonances.[48] The selected resonances are known to decay very selectively into the next lowest ionic vibrational level.[73,74] The measurements are shown in Fig. 5 and compared with the REMPI state-selection experiments by Gerlich,[75] quantum scattering studies by Gilibert *et al.*[70] and Huarte-Larrañaga *et al.*,[71,72] and QCT calculations carried out by Zhang *et al.*[48] using the same 3D potential energy surface developed by Pendergast *et al.*[52] that was used in the quantum scattering studies.

In the QCT calculations, only those reactive channels are included in the cross section determination that lead to product molecular ions with vibrational energy exceeding the zero-point energy. Failure to do so results in nonzero prethreshold cross sections, although an apparent improved agreement with near-threshold experimental values was noted by Urban *et al.*[68] The latter comparison, however, is fortuitous and does not take into account that the experimental measurements by Gerlich, as well as those by Zhang *et al.*, are kinematically broadened, leading to prethreshold signal (arrows in Fig. 5 indicate the thresholds of the respective experiments). A proper comparison between theory and experiment needs to take into account the experimental broadening stemming from the ion energy resolution (≈0.3 eV in

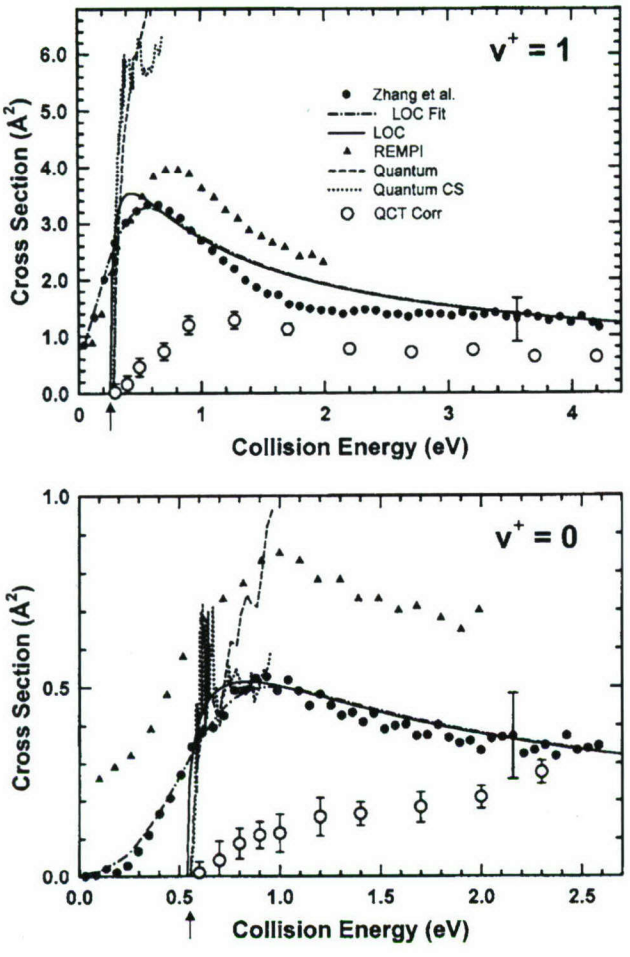

FIG. 5. Collision energy (center of mass) dependence of $H_2^+(v^+=0,1)+Ne$ proton transfer cross sections. Experimental cross sections are from Zhang *et al.* (Ref. 48) (filled circles) and Gerlich (Ref. 68) (filled triangles). Theoretical work includes quantum scattering work by Gilibert *et al.* (Ref. 70) (quantum CS, dotted line) and Huarte-Larrañaga *et al.* (Refs. 71 and 72) (quantum, dashed line), and quasiclassical trajectory calculations by Zhang *et al.* (Ref. 48). The dashed-dot line is a fit of the modified line-of-centers model [Eq. (5), LOC] convoluted by the experimental energy broadening mechanisms to the experimental cross sections by Zhang *et al.* The solid lines are the deconvoluted modified LOC cross sections. Taken from Ref. 48.

the laboratory frame of reference) and thermal target gas motion. Figure 5 also shows the kinematically deconvoluted experimental cross sections (solid lines), which are obtained from a nonlinear least-squares fit of the modified line-of-centers (LOCs) threshold function,[76,77]

$$\sigma = A\frac{(E_T + E_i - E_0)^n}{E_T}, \tag{5}$$

convoluted by the energy broadening factors of the experiment, to the experimental data. In Eq. (5), E_T is the center-of-mass translational or collision energy, A is a scaling parameter, $E_0=0.54$ eV is the threshold energy, E_i is the internal energy above the zero-point energy, and n is the curvature parameter. The primary contribution to broadening at low energies is the primary ion beam resolution. Satisfactory fits of the threshold behavior are obtained when fixing the threshold, E_0-E_i. Very low curvature parameters of 0.353 and 0.390 are determined from the fit for $v^+=0$ and 1, respectively, resulting in the very sharp thresholds of the deconvoluted curves that are in agreement with the behavior observed in the quantum scattering calculations.

The low curvature parameters are close to $n=0.5$ predicted for a complex formation mechanism[76] with a reverse exothermic reaction governed by a Langevin-Gioumousis-Stevenson capture mechanism.[78] Crossed-beam experiments by Bilotta and Farrar, however, show little evidence in the angular scattering distributions for complex formation at energies as low as 0.87 eV.[79] The poor agreement with the QCT calculations near threshold, on the other hand, suggests that quantum effects play an important role. This is consistent with the observation of a dense resonance structure in the quantum studies. While the quantum scattering studies of Gilibert *et al.*[70] based on the coupled-state approximation are in good agreement with experiment for $v^+=0$, the exact quantum scattering results of Huarte-Larrañaga *et al.*[71,72] are significantly higher above threshold. Both quantum scattering results for $v^+=1$ overshoot the observed cross sections above threshold. The discrepancy with experiment suggests that the quantum scattering calculations may be overemphasizing the effects of resonances, which could be attributed to inaccuracies in the interaction potential.

Figure 6 compares the vibrationally state-selected integral absolute cross sections for the $H_2^+(v^+)+Ne$ system at three collision energies determined in PFI-PESICO measurements with those obtained by QCT calculations. In all charts a rapid increase of the proton-transfer cross sections is observed with vibrational energy. At a translational energy of 0.7 eV, cross sections could be measured for $v^+=0-17$. At low vibrational energies, the cross sections are higher than the QCT predictions. Above $v^+=3$, the agreement between measured and calculated cross sections is very satisfactory. At the highest reactant vibrational energies, the cross section declines with vibrational energy, most likely due to competition with the CID cross section. The QCT CID cross sections are also shown. The ion guide trapping field was insufficient to capture reliably fast CID product protons. The CID channel is open above $v^+=8$. In the high vibrational energy range where CID is competitive, the agreement between the measured and QCT cross sections is again not optimal.

At a translational energy of 1.7 eV, the agreement between measured and QCT cross sections is significantly better at low vibrational energies. At the highest measured levels, there is again poorer agreement. At 4.5 eV, there is poor agreement between the measured values and the QCT results. The data can be summarized as identifying three energy regions, $E_{tot}=E_T+E_i$: a low energy region below total energies of 1.5 eV, at which quasiclassical theory underpredicts cross sections, most likely due to the importance of quantum effects; an intermediate region, $1.5<E_{tot}<3$ eV, where the agreement between quasiclassical predictions and experiment is excellent; and a high energy region, $E_{tot}>3$ eV, where quasiclassical theory again underpredicts the cross sections. The discrepancy at high energies may be as-

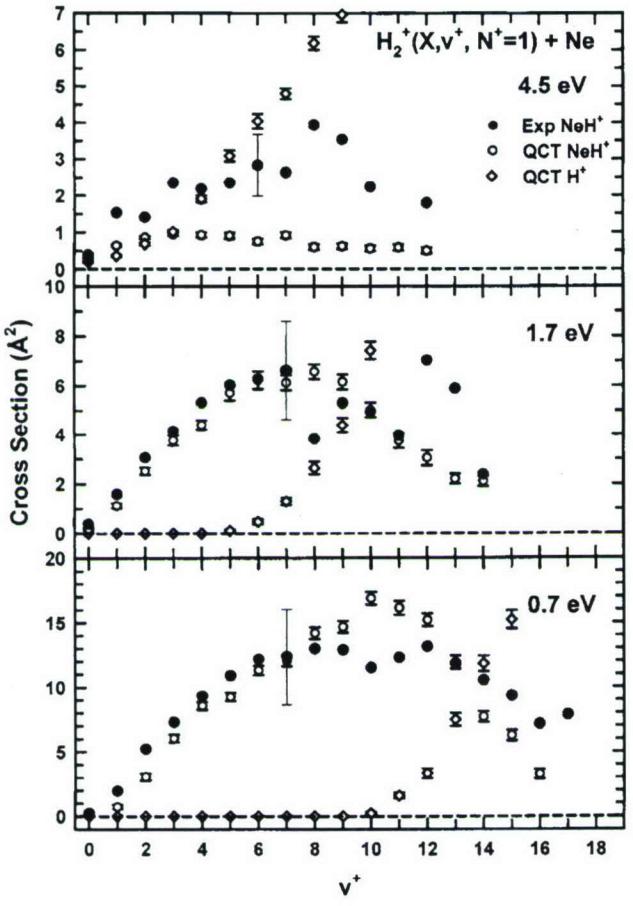

FIG. 6. PFI-PESICO measurements by Zhang *et al.* (Ref. 48) (filled circles) of $H_2^+(v^+, N^+=1)+Ne$ proton-transfer cross sections as a function of vibrational quantum number (v^+) at three translational energies, E_T=0.7, 1.7, and 4.5 eV. The error bars (±30%) for the experimental cross sections represent the maximum absolute errors. The experimental results are compared with QCT calculations by Zhang *et al.* of the proton transfer and dissociation cross sections including zero-point energy restrictions. Taken from Ref. 48.

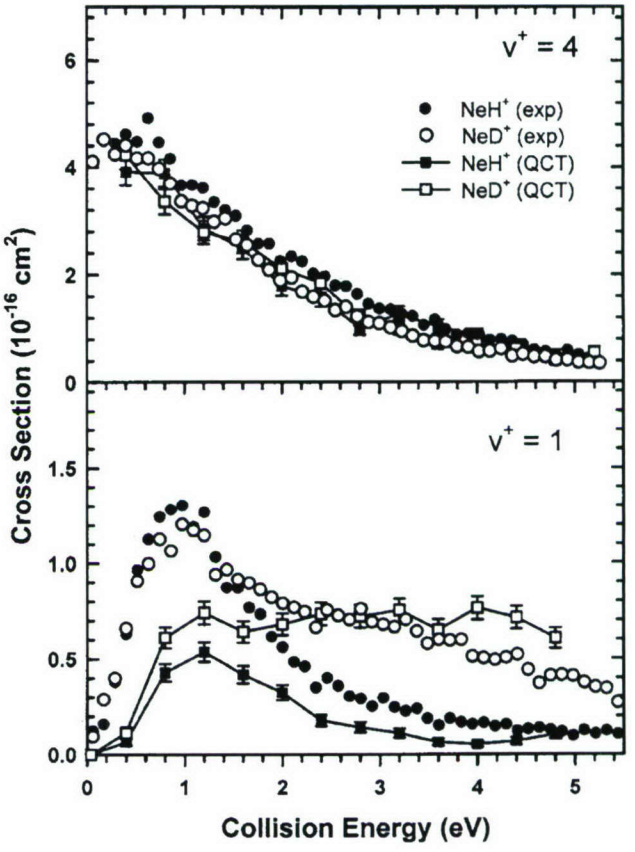

FIG. 7. Collision energy (center of mass) dependence of state-selected $HD^+(v^+=1,4)+Ne$ isotopic reaction channel cross sections. The results are compared to QCT calculations by Tang *et al.* (Ref. 81).

sociated with an overprediction of CID cross sections and the associated competition. In the H_2^++He systems, discussed later, classical trajectory hopping studies have shown that nonadiabatic electronic transitions play an important role in the CID channel.[80] Consequently, classical theory may fail to correctly portray the dynamics at high energies. Inaccuracies in the potential developed by Pendergast *et al.*[52] may also be a possible cause.

Isotope effects represent a particularly sensitive test of interaction potentials. Figure 7 shows very recent measurements[81] of the translational energy dependence of the HD^++Ne proton-transfer reaction cross section:

$$HD^+ + Ne \rightarrow NeH^+ + D \quad \Delta H = 0.55 \text{ eV} \tag{6}$$

$$\rightarrow NeD^+ + H \quad \Delta H = 0.50 \text{ eV} \tag{7}$$

for both isotopic channels measured for reactant vibrational quanta $v^+=1$ and 4. The endothermicities are based on recent theoretical work on NeH^+/NeD^+ by Civis *et al.*[82] While the $HD^+(v^+=1)+Ne$ proton-transfer channels are endothermic:

$$HD^+(v^+=1) + Ne \rightarrow NeH^+ + D \quad \Delta H = 0.29 \text{ eV} \tag{8}$$

$$\rightarrow NeD^+ + H \quad \Delta H = 0.25 \text{ eV}, \tag{9}$$

both $HD^+(v^+=4)+Ne$ channels are exothermic. The measurements were again conducted in a noncoincidence, autoionization mode. The results are compared to QCT calculations conducted on the surface by Pendergast *et al.*[52] In the $v^+=1$ case, the experimental data exhibit no isotope effects at collision energies below 2 eV, despite the difference in threshold. At higher energies, a large isotope effect in favor of NeD^+ is observed. Contrary to the experiments, QCT predictions favor the NeD^+ channel already near threshold. As in the H_2^+ reaction, the absolute QCT cross sections are considerably smaller than the observed values at low energies. These differences can again be explained by important quantum effects at low energies, possibly longer-lived quantum resonances, which appear to scramble isotopic preferences, observed in more direct scattering dynamics. At higher energies, the experiments clearly reveal an isotope effect, the magnitude of which approaches the QCT predictions with increasing translational energy. A generally similar behavior is observed for $v^+=2$ and 3.

For $v^+=4$, both QCT cross sections and experimental results exhibit no evidence of isotope effects within the computational and experimental uncertainties. The superb agreement between the experimental results and the QCT calcula-

tions at all investigated translational energies demonstrates nicely that above internal energies of ~1 eV [the pure vibrational energy of $HD^+(v^+=4)$ is 1.0 eV] classical theory performs very well. The declining cross section with energy suggests a longer-range interaction, typical of exothermic ion-molecule reactions with spectator-stripping-type dynamics. In the $v^+=1$ case (Fig. 7), the transition at which quantum effects no longer affect the integral cross section occurs at higher total energies in this endothermic reaction system, where average impact parameters are significantly smaller.

C. The $H_2^+, HD^+(X, v^+)$+He proton-transfer system

The H_2^++He proton-transfer system

$$H_2^+ + He \rightarrow H + HeH^+, \quad \Delta H = 0.806 \text{ eV} \tag{10}$$

is arguably the most thoroughly studied ion-molecule reaction. Due to the significant endothermicity, considerable vibrational effects are expected and it was for this reaction that Chupka *et al.* discovered the first vibrational effects in an ion-molecule reaction in their pioneering photoionization studies.[22–24] Koyano and co-workers[11,63] and Govers and Guyon[4] used the threshold photoelectron coincidence approach to measure relative proton-transfer cross sections for low $H_2^+(v^+<7)$ reactant states. The latter derived absolute cross sections based on the phenomenological cross sections of Chupka *et al.*[22–24] Turner *et al.* determined absolute integral cross sections for this reaction as well as the HD^++He system in a well-characterized guided-ion beam experiment in which the reactant ions were efficiently prepared in selected vibrational states $v^+=0-4$ using monochromatic VUV photoionization through autoionization resonances.[8] The detailed results portrayed a picture of low-impact parameter intimate dynamics for the lowest reactant level, $v^+=0$, while the results at higher levels appeared consistent with a spectator-stripping mechanism.[59,60]

Given its fundamental importance, the H_2^++He system has been the subject of numerous theoretical studies including QCT (Refs. 80 and 83–92) and quantum scattering calculations of collinear[93–102] and 3D zero total angular momentum[69,99,103–106] ($J=0$) reaction probabilities and integral cross sections.[69,107,108] Theoretical studies have received a new impetus from a recent, high-quality three-dimensional potential energy surface developed by Palmieri *et al.*[51] The surface prompted new quantum scattering calculations at arbitrary J.[50,51,109–111] As in the H_2^++Ne case, the quantum mechanical studies revealed a dense resonance structure in the J-resolved reaction probabilities.

Tang *et al.* conducted an in-depth study of the $H_2^+(v^+)$ +He proton-transfer system for reactant states as high as $v^+=15$.[49] The translational energy dependence of the state-selected proton-transfer cross sections at low v^+ states were determined using the same autoionization approach applied in the measurements of Fig. 5. The measurements for $v^+=1$, 2, and 3 are shown in Fig. 8, where they are compared with the experimental measurements of Turner *et al.*,[8] the most recent quantum scattering studies, as well as QCT results. For $v^+=1$, the measurements of Tang *et al.* are very comparable to the earlier measurements by Turner *et al.* in absolute magnitude, the latter having a more gradual onset which is most likely attributable to a lower translational energy resolution. Tang *et al.* modeled their data using the modified LOC model [Eq. (5)] and the deconvoluted results are shown in Fig. 8. As in the case of the H_2^++Ne system, the curvature parameter determined from the fit is very small, $n=0.36$, signifying a sharp onset at threshold. This sharp threshold behavior is again not reflected in the QCT cross sections, performed on the surface by Palmieri *et al.*,[51] which show a gradual increase above threshold that eventually approaches the measured values near 2 eV.

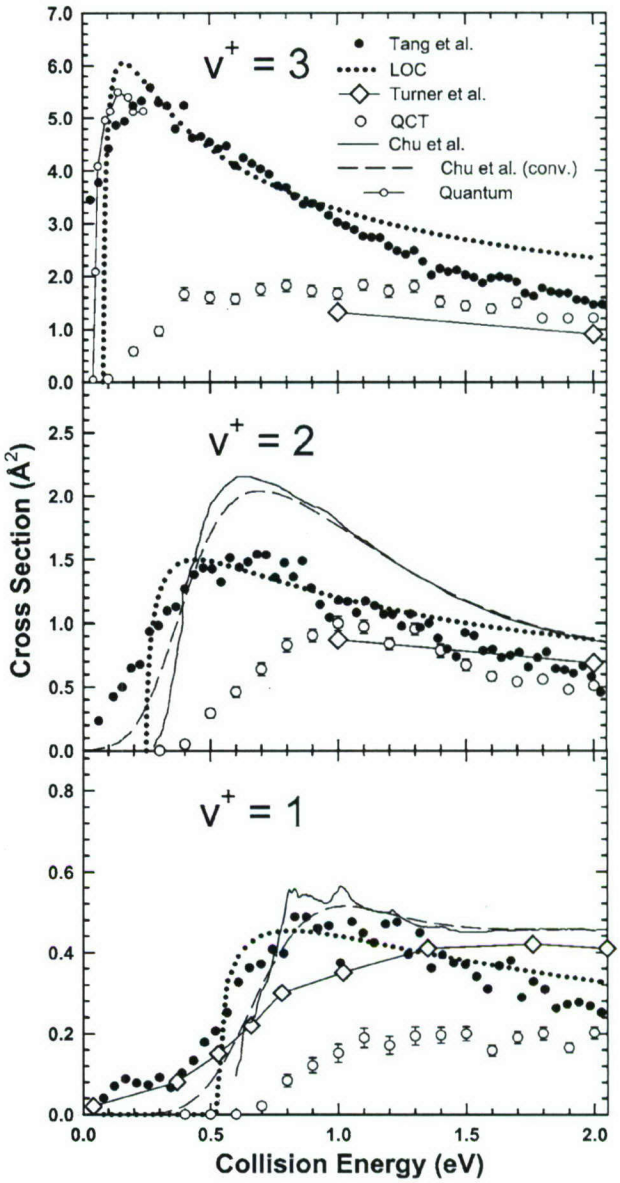

FIG. 8. Collision energy (center of mass) dependence of $H_2^+(v^+=1-3)$ +He proton-transfer cross sections. Experimental cross sections are from Tang *et al.* (Ref. 49) (filled circles) and Turner *et al.* (Ref. 8) (open diamonds). LOC (dotted lines) refer to the modified line-of-centers model fits of the cross sections of Tang *et al.* The experimental measurements are compared with QCT calculations (open circles), and quantum scattering work by Chu *et al.* (Ref. 110) (solid lines), and Aquilanti *et al.* (Ref. 50) (Quantum). The dashed lines are the theoretical results of Chu *et al.* convoluted by the energy broadening mechanisms of the experiment by Tang *et al.* (Ref. 49).

The sharp threshold onset is also observed in quantum scattering studies,[50,107,108] which exhibit significant structure in the energy dependence that are attributed to quantum scattering resonances. Since Tang *et al.* published their results, Panda and Sathyamurthy[111] and Chu *et al.*[110] conducted time-dependent quantum scattering studies using the surface by Palmieri *et al.*[51] The results of Chu *et al.* are shown in Fig. 8. They conducted calculations over a significantly broader collision energy range than all previous quantum scattering work and explicitly incorporated Coriolis coupling. The latter was shown to have an important effect on the integral cross sections. The cross sections of Chu *et al.* are in very satisfactory agreement with the experimental measurements of Tang *et al.*. Interestingly, the quantum scattering cross sections do not show as vertical an onset as derived from the modified LOC deconvolution. Since the modified line-of-centers model is not suited for mimicking theoretical threshold behavior, we have convoluted the results by Chu *et al.* with the broadening factors of the ion beam experiment of Tang *et al.* (ion energy resolution, thermal target gas motion) to compare more appropriately with the experimental results. The convoluted theoretical values (dashed curve) have a slope above threshold that is very similar to that of the experiment, except that they are shifted by ~0.1 eV to higher values. Due to the small magnitude in cross section, the experiment by Tang *et al.* may have been affected by secondary collisions, causing a slight shift in the appearance of the threshold to lower values. The effect of secondary collisions is significantly more apparent for $v^+=0$ reactants, where the cross sections are much smaller.[49]

For $v^+=2$, the situation is very similar. Again, the absolute cross sections measured by Tang *et al.* and Turner *et al.* are in good agreement, the modified LOC model derives a small curvature parameter, $n=0.44$, and the QCT comparison is poor near threshold, but excellent above 1 eV. The maximum of the cross sections calculated by Chu *et al.* is about 30% higher than the measured values, which is within the quoted errors of the experiment. As for $v^+=1$, the convoluted theoretical onset is slightly shifted from the experimental onset. The cross sections measured by Tang *et al.* for $v^+=3$ were shown to be in excellent agreement with the phenomenological cross sections derived by Chupka and *et al.*[22–24] It is seen in Fig. 8 that they are approximately a factor of 2 higher than the measurements of Turner *et al.*.[8] Again, there is a marked difference between experiment and QCT calculations, the convergence of the two happening at higher energies than for $v^+=2$. Chu *et al.* did not calculate the translational energy dependence for this reactant state. The figure compares the experimental data with calculations by Aquilanti *et al.*[50] based on the Palmieri surface. Apart from a slight difference between the onsets of modified LOC deconvoluted experimental and quantum scattering cross sections that can be attributed to experimental uncertainty, the experimental and theoretical cross sections are in excellent agreement. Time-dependent quantum scattering studies[108] on an older surface derived by Joseph and Sathyamurthy[90,91] also produced good agreement with the experimental measurements for the $v^+=3$ reactant state.

Tang *et al.* measured state-selected PFI-PESICO cross sections at translational energies of 0.6 and 3.1 eV.[47] Figure 9 compares their measurements to other experiments as well as QCT calculations conducted on the Palmieri surface. At 0.6 eV, Tang *et al.* succeeded in measuring cross sections with good coincidence statistics for $v^+=1-15$. The measurements with estimated absolute errors of ±40% compare well to scaled relative cross sections by Koyano and co-workers[11,63] for $v^+=1-4$. The QCT calculations underestimate the cross section up to $\sim v^+=7$, corresponding to a vibrational excitation energy of 1.59 eV. At higher reactant states, the agreement with the trajectory calculations is excellent. Even the cross section decline with vibrational quantum state that is attributable to competition with the dissociation channel, for which the QCT calculations are also shown, is nicely reproduced by the QCT calculations.

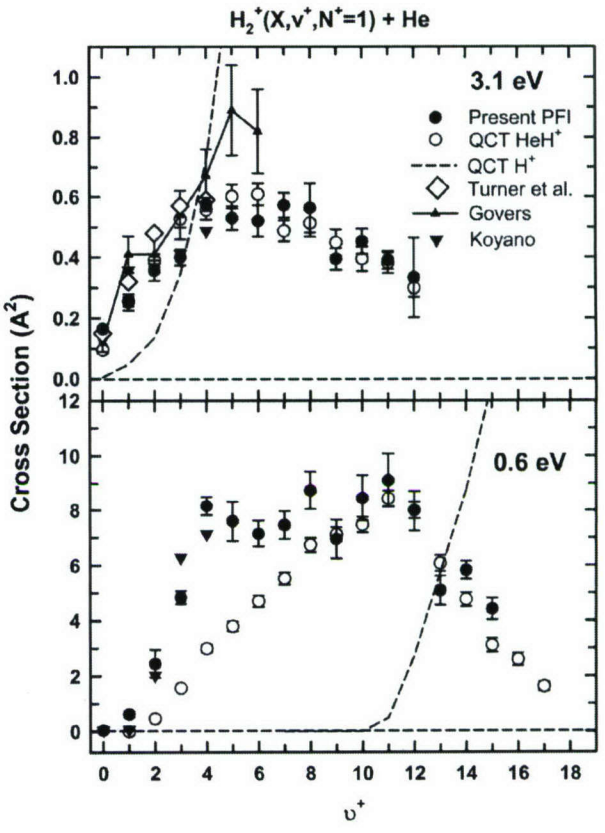

FIG. 9. PFI-PESICO measurements by Tang *et al.* (Ref. 49) (filled circles) of $H_2^+(v^+,N^+=1)+He$ proton-transfer cross sections as a function of vibrational quantum number (v^+) at two translation energies, $E_T=0.6$ and 3.1 eV. The PFI-PESICO errors bars represent statistical errors. The experimental results are compared with experimental results by Turner *et al.* (Ref. 8) (open diamonds), Govers and Guyon (Ref. 4) (upward pointing filled triangles), and Koyano and co-workers (Refs. 11 and 63) (downward pointing filled triangles). The measurements of Turner *et al.* are the averages of measurements at $E_T=2$ and 4 eV. QCT calculations by Tang *et al.* (Ref. 49) of the proton transfer (open circles) and dissociation (dashed lines) cross sections including zero-point energy restrictions are also shown.

At 3.1 eV, experimental cross sections were obtained for $v^+=1-12$. Scaled relative cross sections for $v^+=1-4$ by Koyano and co-workers[11,63] taken at 3.0 eV are again in good agreement with the PFI-PESICO results. Relative cross section measurements by Govers and Guyon[6] for $v^+=0-6$ scaled to the phenomenological cross sections of Chupka *et*

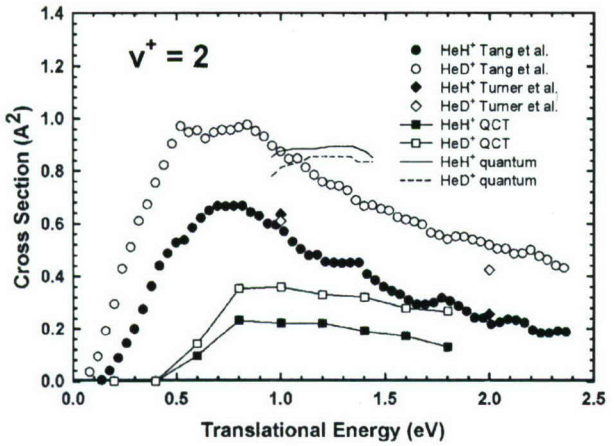

FIG. 10. Collision energy (center of mass) dependence of $HD^+(v^+=2)$ +He isotopic reaction channel cross sections. The results by Tang *et al.* (Ref. 81) (circles) are compared to experiments by Turner *et al.* (Ref. 8) (diamonds) and QCT calculations by Tang *et al.* (Ref. 81) (squares). Also shown are recent quantum scattering calculations by Tiwari *et al.* (Ref. 109).

al.[22–24] are also in satisfactory agreement with the PFI-PESICO measurements. We also show experimental cross sections of Turner *et al.*[8] for $v^+=0-4$ consisting of the average of their $E_T=2$ and 4 eV measurements. The use of an average for comparison is justified given the close to linear drop in cross section observed for all reactant states at the respective translational energies. The resulting cross sections are also in good agreement with the PFI-PESICO measurements. Unlike the observations in the H_2^++Ne system discussed earlier, the QCT calculations are in excellent agreement with the state-selected measurements at these relatively high total energies. This suggests that either the H_2^++He surface is more accurate, or that nonadiabatic effects encountered at energies near the dissociation limit play a role in the H_2^++Ne system, but are weak in the He reaction.

Isotopic cross sections of the HD^++He system have been measured recently.[81] Figure 10 shows sample isotopic proton-transfer cross sections for the reaction $HD^+(v^+=2)$ +He:

$$HD^+(v^+=2)+He \rightarrow HeH^+ + D \quad \Delta H = 0.36 \text{ eV} \qquad (11)$$

$$\rightarrow HeD^+ + H \quad \Delta H = 0.32 \text{ eV}. \qquad (12)$$

The thresholds were derived using the HeH^+/HeD^+ zero-point energies obtained from Coxon and Hajigeorgiou.[112] Tang *et al.* observe a significant isotope effect from threshold to 2 eV. The absolute cross section measurements by Turner *et al.*[8] are in good agreement with the measurements of Tang *et al.* at 2 eV. However, at 1 eV, they do not observe an isotope effect, although the absolute cross sections are in good agreement with the HeH^+ cross section of Tang *et al.*. The QCT calculations correctly predict the isotope effect observed by Tang *et al.*, although the magnitude of the HeD^+/HeH^+ cross section ratio is slightly underpredicted. Very recently, high-level time-dependent quantum mechanical calculations have been conducted by Tiwari *et al.*[109] on the isotopic branching in this reaction. The potential by Palmieri *et al.*[51] was used. The calculated integral cross sections for the state-selected reactions (11) and (12) are also shown in Fig. 10. Although the absolute values of the integral cross sections are comparable to the experimental values, the energy dependence of the cross sections, as well as the isotope effects, are not correctly rendered.

IV. CONCLUSIONS AND OUTLOOK

A. VUV synchrotron based PFI-PESICO measurements

The described state-selected studies of H_2^+ proton-transfer reactions that build on the pioneering work of Chupka *et al.*[22–24] and Lee and co-workers[7,8] provide new validation opportunities for state-of-the-art reaction dynamics theory covering a significantly broader range of energy space. As the comparison of these recent experimental results with the most exact theoretical approaches demonstrates, there are still important discrepancies in the determined reaction cross sections for the H_2^++He and H_2^++Ne systems at low total energies, even though the dynamics can be considered to unfold on a single potential energy surface. The comparison to QCT calculations exhibits a distinct transition between dynamics governed by quantum effects at low vibrational and translational energies to dynamics at higher vibrational and/or translational energies, where quantum effects average out and where QCT correctly renders the energy dependence of reaction cross sections. The present PFI-PESICO work has provided a rare opportunity to observe this transition for the vibrational energy of the reactant ions of an ion-molecule reaction.

The H_2^++He and H_2^++Ne systems also provide a rare opportunity to study a system where theory has identified quantum scattering resonances that not only affect J-resolved scattering probabilities, but also greatly affect the resulting integral cross sections. As seen in Fig. 5, marked resonance structure near threshold is predicted by the coupled-state calculations of Gilibert *et al.*[70] of the $H_2^+(v^+=0)$+Ne integral proton-transfer cross section. The absolute magnitude of the cross sections are in excellent agreement with the measurements by Zhang *et al.*.[48] Although both the experiments by Zhang *et al.*[48] and Gerlich[68] exhibit the hint of a shoulder at energies where the calculated cross sections exhibit maxima due to resonances, the confirmation of these resonance structures would require a higher translational energy resolution of the guided-ion beam experiments. An improved translational energy resolution would also allow the observation of the effects due to the rotational state of the reactant ion. While the PFI-PESICO experiment has demonstrated the ability to select single rovibrational states of H_2^+, the low translational energy resolution makes it all but impossible to conduct measurements precisely near threshold, where rotational effects are most likely. The possibility of rotational effects has been predicted by Chu *et al.* for the H_2^++He system[110] using a time-dependent wave packet calculation that includes Coriolis coupling.

The challenges of improving the kinetic energy resolution in ion-molecule collisional experiments have been discussed previously.[46] Two obvious experimental improvements involve the narrowing of the reactant ion beam kinetic energy spread and the reduction of thermal broadening of the

neutral reactants due to the Doppler effects.[113] The former improvement can be partly accomplished by minimizing the stray field due to surface defects of the metal electrodes used in the photoionization region together with lowering the extraction electric field for the reactant ions. However, the lowering of the ion extraction field can seriously lower the reactant ion intensity and thus be detrimental to the ion-molecule collisional experiment. Furthermore, the ion kinetic energy can be broadened by improper ion injection into the rf octopole ion guide,[30] when the ion guide reaction gas cell arrangement is used. Lowering the thermal broadening of reactant neutrals has been achieved by either cooling the collision cell[114,115] or replacing the cell with a supersonic[114,116–118] jet, which also comes with a sizeable penalty in the signal-to-noise ratio of the collisional experiments. The broad kinetic energy distribution also limits the lowest meaningful collision energy of the experiment. The best ion energy resolution in a guided-ion beam experiment has been obtained by Gerlich, where a quadrupole velocity filter was used to narrow the distribution to ≈50 meV [full width at half maximum (FWHM)].[30] Since this resolution is still significantly higher than the rotational constants of H_2^+, the observation of the rotational effect in ion-molecule collisions is expected to be difficult.

Despite the limitation of achievable kinetic energy resolution, the VUV synchrotron PFI-PESICO technique can be readily employed for state-selected absolute integral cross section measurements of ion-molecule reactions of other diatomic, triatomic, and simple polyatomic molecular ions. Rotationally resolved PFI-PE vibrational bands for $O_2^+(X\,^2\Pi_{3/2,1/2}, v^+=0-38)$,[119] $O_2^+(a\,^4\Pi_{5/2,3/2,1/2,-1/2u}, v^+=0-18)$,[120] $NO^+(X\,^1\Sigma^+; v^+=0-32)$,[121] $NO^+(a\,^3\Sigma^+; v^+=0-16)$,[122] and $CO^+(X\,^2\Sigma^+, v^+=0-42)$ (Ref. 123) have been observed in recent VUV synchrotron measurements. The vibrational bands for $v^+=0-8$ and 0–67 of $N_2^+(X\,^2\Sigma_g^+)$ have also been observed in previous VUV laser PFI-PE (Ref. 124) and synchrotron based threshold photoelectron[125] studies, respectively. The high-resolution nature of the PFI-PESICO method would allow the examination of the reactivity of individual spin-orbit and high v^+ levels of these ions. For example, a study to compare the reaction cross sections involving near resonance $O_2^+(X\,^2\Pi_{3/2,1/2}, v^+)$ and $O_2^+(a\,^4\Pi_{5/2,3/2,1/2,-1/2u}, v^+)$ states, such as the $O_2^+(X\,^2\Pi_{3/2,1/2}, v^+=28)$ and $O_2^+(a\,^4\Pi_{5/2,3/2,1/2,-1/2u}, v^+=8)$ states and the $O_2^+(X\,^2\Pi_{3/2,1/2}, v^+=29)$ and $O_2^+(a\,^4\Pi_{5/2,3/2,1/2,-1/2u}, v^+=9)$ states, would be interesting and promise to provide new insight into the reactivity of ions in highly excited vibrational and spin-orbit states.

B. Development of the VUV laser based PFI-PI technique

By using two-photon laser PFI-PI or mass analyzed threshold ion techniques, Mackenzie and Softly[126] and Green *et al.*[127] have previously examined the rotational energy effects in the $H_2^+(v^+=0, N^+=0-4)+H_2$ and the $NO^+(v^+=0, N^+)+C_2H_5I$ reactions. The two-color UV laser PFI-PI schemes for the preparation of state-selected ions are limited to the existence of stable intermediate states in the UV, whereas the VUV-PFI-PI scheme does not suffer from this limitation, and is generally applicable to all states resolved in the PFI-PE spectrum of a molecular ion. It has been shown that by using four-wave sum- and difference-frequency mixing schemes in Ar, Kr, Xe, and Hg as the nonlinear media, tunable coherent VUV laser radiation with optical bandwidth of 0.12 cm^{-1} (FWHM) can be generated in the full energy range of 7–19.5 eV.[128–130] While the ease of VUV tunability remains a great advantage of synchrotron sources, the significantly higher energy resolutions offered by VUV lasers are expected to provide higher photoionization selectivity for the preparation of reactant ion states.

Recently, Ng and co-workers have converted their triple-quadrupole-double-octopole (TQDO) photoionization ion-molecule reaction apparatus[2,25] in their laboratory to a VUV laser based ion-molecule reaction apparatus.[131] This involves the replacement of the VUV discharge lamp system by a comprehensive tunable VUV laser system and the implementation of a sensitive VUV laser PFI-PI scheme for the preparation of state-selected reactant ions. The key for the success is to generate a sufficiently high intensity of PFI-PIs by increasing the VUV laser pulse energy along with lengthening the lifetimes of excited high-n Rydberg states by employing a scrambling field[132,133] scheme.

By using a MgF_2 lens instead of a windowless VUV monochromator to separate the fundamental frequencies from the VUV difference frequency, Ng and co-workers have measured a VUV laser pulsed energy of ≈10 μJ at 9.26 eV or a photon intensity of $\approx 2\times10^{14}$ photons/s for a 30 Hz laser as compared to that of 10^9-10^{11} photons/s observed at the ALS high-resolution (resolution ≈1–5 cm^{-1}, FWHM) VUV synchrotron source. This increase in VUV laser intensity observed by eliminating the monochromator is critically important for the success of using the VUV-PFI-PI scheme for the preparation of state-selected reactant ions. For VUV wavelengths shorter than 1050 Å (absorption cutoff of LiF), a convex LiF lens can no longer be used to separate the VUV from fundamental frequencies. Recently, it has been shown that this can be overcome by intersecting the two dye laser beams at a slight angle onto a rare gas free jet, such that the VUV beams of sum and difference frequencies would emerge in directions different from those of the fundamental laser beams.[134] This arrangement, which allows the selection of the VUV beam of interest by using a slit without using a monochromator or a convex lens, can also be implemented for the generation of VUV laser radiation at wavelengths shorter than 1050 Å.

For PFI-PI detection using pulsed (30 Hz) VUV lasers, PFI-PIs formed from PFI of high-n Rydberg species must be separated from prompt background ions using a dc separation field and an appropriate time delay between the application of the VUV laser pulse and the pulsed electric field for PFI and ion extraction.[39] The time delay requirement demands long lifetimes for the high-n Rydberg states. Schlag and co-workers[132,133] and Kim and co-workers[135,136] have demonstrated that using a small scrambling electric field during the laser excitation to promote the Stark mixing to high orbital angular momentum l states from low l states origi-

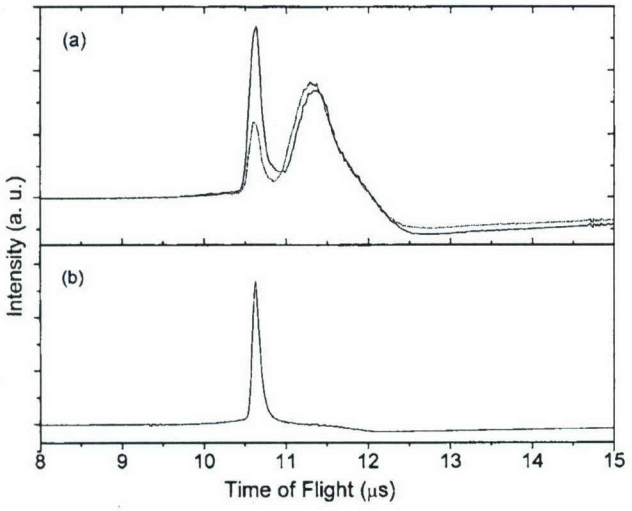

FIG. 11. (a) TOF spectrum showing the NO^+ PFI-PI and prompt background ion peaks (observed using an oscilloscope). The spectra were obtained with the VUV set at the IE[$NO \rightarrow NO^+(v^+=1)$]. The solid and dot curves correspond to the measurements with and without the ringing scrambling electric field, respectively. (b) TOF spectrum showing the NO^+ PFI-PI peak after the prompt NO^+ background peak was blocked by a pulsed electric field applied to the lower repeller plate. Taken from Refs. 131 and 137.

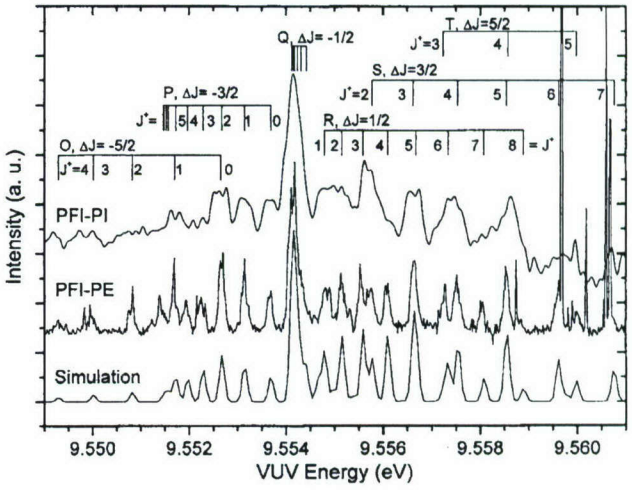

FIG. 12. Comparison of the rotational-resolved PFI-PE spectrum (middle), the PFI-PI spectrum (upper), and the simulated (bottom) spectra for $NO^+(X,v^+=1,J^+) \leftarrow NO(X,v''=0,J'')$. The spectral simulation gives a rotational temperature of 50 K for NO. Taken from Refs. 131 and 137.

nally formed in laser excitation can significantly lengthen the Rydberg lifetimes and thus enhance the PFI-PI signal.

As an example, we show in Fig. 11(a) the TOF spectra for PFI-PI and prompt background NO^+ ions observed in the VUV PFI detection of NO with the VUV laser energy set at the ionization energy (IE) for the formation of $NO^+(X,v^+=1)$ from NO.[131] The delay of the PFI field pulse with respect to VUV laser pulse is 5 μs and the dc separation field and the PFI field are 0.5 and 6 V/cm, respectively. As a result of the application of the dc separation field and the delay of the PFI electric field pulse, the PFI-PI peak (10.50 μs) is well separated from the prompt background ion peak (11.25 μs). The solid and dot spectra of Fig. 11(a) correspond to the respective measurements observed with and without the ringing scrambling electric field. The PFI-PI intensity is found to increase by more than a factor of 3 by using the scrambling field. As expected, the prompt background ion intensity is independent of the scrambling field. The enhancement factor for the PFI-PI intensity is found to vary in the range of 3–5 depending on the selected rovibrational state of $NO^+(X)$. In order to use the PFI-PIs formed for state-selected ion-molecule reaction studies, it is necessary to reject the background prompt ions. The prompt background ions can be effectively blocked by applying an appropriate voltage pulse to the photoionization region after the PFI-PIs exit the photoionization region on the way to the ion detector. As shown in Fig. 11(b), the TOF spectrum only reveals the PFI-PI peak when the blocking voltage pulses are applied to the lower repeller plate at the appropriate delay with respect to the PFI pulses.

Figure 12 compares the rotationally resolved PFI-PE (middle) and PFI-PI (top) spectra of $NO^+(X;v^+=1)$ obtained using a neat NO beam.[131,137] The simulated spectrum (bottom curve of Fig. 12) is obtained assuming a rotational temperature of 50 K. Due to the higher PFI voltage used in the PFI-PI measurement, the energy resolution (3 cm^{-1}, FWHM) for the PFI-PI spectrum is lower than that (1.5 cm^{-1}, FWHM) of the PFI-PE spectrum. Nevertheless, the $J^+=0-2$ states of $NO^+(X;v^+=1)$ are still clearly resolved. A PFI-PI intensity of $(1-5)\times10^4$ ions/s was found to be readily obtainable for NO^+ in $v^+=0$, 1, or 2 state.

As a demonstration experiment, Chang *et al.* have obtained absolute total charge-transfer cross sections for $NO^+(X;v^+=0-2)+CH_3I$ collisions at center-of-mass collision energies of 0.5–5.0 eV by implementing the VUV laser PFI-PI method in the TQDO apparatus.[137] As expected, the CH_3I^+ charge-transfer cross sections are sensitive to the $NO^+(v^+)$ state, but not to the collision energy. The observed CH_3I^+ cross sections for $NO^+(X;v^+=0,1,$and 2) are found to be $\approx$1, 10, and 20 Å^2, respectively, and are essentially constant in the collision energy range of 0.5–5.0 eV. The high cross sections observed for the $NO^+(X;v^+=1$ and 2) $+CH_3I$ charge-transfer reactions are consistent with the fact that IE[$NO \rightarrow NO^+(v^+=2)$]=9.84 eV > IE[$NO \rightarrow NO^+(v^+=1)$]=9.55 eV $\approx$ IE(CH_3I)=9.54 eV,[121,138] i.e., these charge-transfer reactions are exothermic. Because the charge-transfer collision for $NO^+(v^+=0)+CH_3I$ is endothermic by 0.26 eV, charge transfer is translationally driven, leading to a small charge-transfer cross section of $\approx$1 Å^2.

The success in the application of the high-resolution VUV laser PFI-PI method for state-selected ion-molecule reaction studies promises many exciting developments to come. The pulsed nature of the PFI-PI beam generated by the VUV laser PFI-PI method would favor the experiment to be conducted in a crossed ion-neutral beam arrangement because the neutral reactants can be introduced into the reaction region as a pulsed beam to synchronize with the arrival of the PFI-PI beam pulse. As pointed out above, the beam-beam arrangement is expected to improve the kinetic energy resolution for the ion-neutral collision experiment.[113] Considering that many excellent designs for generating pulsed

radical beams exist,[139,140] the beam-beam arrangement would also make possible the study of state-selected ion-radical reactions, which is essentially a new field.

By virtue of the significant improvement of detection sensitivity, the imaging techniques have played an important role in recent molecular dynamics studies, allowing the angular distributions of state specific product neutrals to be examined in great detail.[141] Up to the present time, only one ion imaging experiment on the angular distribution measurement of ion-molecule collisions has been reported.[142,143] The angular distribution measurements of state-selected ion-neutral collision studies by combining the VUV laser PFI-PI scheme for reactant ion state preparation and ion velocity imaging for product ion detection should be a fruitful endeavor.

ACKNOWLEDGMENTS

This work has been supported by AFOSR through task 2303EP02 and Grant No. F49620-99-1-0234 (Program Manager, Michael R. Berman). One of the authors (C.Y.N.) acknowledges the support of the NSF Grant Nos. CHE-0517871 and ATM-0317422 and the DOE Grant No. DE-FG02-02ER15306 and thanks Professor Y. T. Lee for introducing him into the fascinating fields of VUV chemistry and reaction dynamics. This work is dedicated to the 70th birthday of Professor Yuan T. Lee.

[1] *State-Selected and State-to-State Ion-Molecule Reaction Dynamics*, Advances in Chemical Physics Vol. 82, edited by C. Y. Ng and M. Baer (Wiley, New York, 1992).
[2] C. Y. Ng, J. Phys. Chem. A **106**, 5953 (2002).
[3] T. Baer, in *Gas Phase Ion Chemistry*, edited by M. T. Bowers (Academic, New York, 1979), Chap. 5, pp. 153–196.
[4] T. R. Govers and P.-M. Guyon, Chem. Phys. **113**, 425 (1987).
[5] T. R. Govers, P. M. Guyon, and T. Baer, Z. Phys. D: At., Mol. Clusters **4**, 89 (1986).
[6] T. R. Govers, P. M. Guyon, T. Baer, and K. Cole, Chem. Phys. **87**, 373 (1984).
[7] S. L. Anderson, T. Turner, B. H. Mahan, and Y. T. Lee, J. Chem. Phys. **77**, 1842 (1982).
[8] T. Turner, O. Dutuit, and Y. T. Lee, J. Chem. Phys. **81**, 3475 (1984).
[9] D. V. Pijkeren, E. Boltjes, J. V. Eck, and A. Niehaus, Chem. Phys. **91**, 293 (1984).
[10] D. V. Pijkeren, J. V. Eck, and A. Niehaus, Chem. Phys. Lett. **96**, 20 (1983).
[11] M. Baer, S. Suzuki, K. Tanaka, I. Koyano, H. Nakamura, Z. Herman, and D. J. Kouri, Phys. Rev. A **34**, 1748 (1986).
[12] R. D. Guettler, J. G. C. Jones, L. A. Posey, and R. N. Zare, Science **266**, 259 (1994).
[13] Y. Chiu, B. Yang, H. Fu, and S. L. Anderson, J. Chem. Phys. **102**, 1188 (1995).
[14] S. L. Anderson, Acc. Chem. Res. **30**, 28 (1992).
[15] R. A. Dressler, D. J. Levandier, S. Williams, and E. Murad, Comments At. Mol. Phys. **34**, 43 (1999).
[16] R. A. Dressler and A. A. Viggiano, in *The Encyclopedia of Mass Spectrometry*, edited by N. M. M. Nibbering (Elsevier, Amsterdam, 2005), Vol. 4, p. 534.
[17] P. M. Banks and G. Kockarts, *Aeronomy Part A* (Academic, New York, 1973), p. 14; (Academic, New York, 1973), p. 257.
[18] A. Dalgarno and J. L. Fox, in *Unimolecular and Bimolecular Ion-Molecule Reaction Dynamics*, Wiley Series in Ion Chemistry and Physics, edited by C. Y. Ng, T. Baer, and I. Powis (Wiley, Chichester, 1994), p. 1.
[19] D. G. Torr and N. Orsini, Planet. Space Sci. **25**, 1171 (1977).
[20] G. A. Bird, *Molecular Gas Dynamics and the Direct Simulation of Gas Flows* (Oxford University Press, Oxford, 1994).
[21] C. Park, *Nonequilibrium Hypersonic Aerothermodynamics* (Wiley, New York, 1990).
[22] W. A. Chupka, in *Ion-Molecule Reactions*, edited by J. L. Franklin (Plenum, New York, 1972), Vol. 1.
[23] W. A. Chupka, J. Berkowitz, and M. E. Russell, *Abstracts of Papers of the Sixth International Conference on the Physics of Electronic and Atomic Collisions* (MIT, Cambridge, 1969), p. 71.
[24] W. A. Chupka and M. E. Russell, J. Chem. Phys. **49**, 5426 (1968).
[25] C. Y. Ng, Adv. Chem. Phys. **82**, 401 (1992).
[26] S. L. Anderson, Adv. Chem. Phys. **82**, 177 (1992).
[27] I. Koyano and K. Tanaka, Adv. Chem. Phys. **82**, 263 (1992).
[28] P.-M. Guyon and T. Baer, in *High Resolution Laser Photoionization and Photoelectron Studies*, Wiley Series in Ion Chemistry and Physics, edited by I. Powis, T. Baer, and C. Y. Ng (Wiley, Chichester, 1995), Chap. 1.
[29] E. Teloy and D. Gerlich, Chem. Phys. **4**, 417 (1974).
[30] D. Gerlich, Adv. Chem. Phys. **82**, 1 (1992).
[31] C.-L. Liao, C.-X. Liao, and C. Y. Ng, J. Chem. Phys. **82**, 5489 (1985).
[32] C.-L. Liao, R. Xu, G. D. Flesch, M. Baer, and C. Y. Ng, J. Chem. Phys. **93**, 4818 (1990).
[33] C.-L. Liao, R. Xu, J.-D. Shao, S. Nourbakhsh, G. D. Flesch, M. Baer, and C. Y. Ng, J. Chem. Phys. **93**, 4832 (1990).
[34] T. Baer, J. Booze, and K. M. Weitzel, in *Vacuum Ultraviolet Photoionization and Photodissociatin of Molecules and Clusters*, edited by C. Y. Ng (World Scientific, Singapore, 1991), p. 259.
[35] C. Y. Ng, Int. J. Mass. Spectrom. **200**, 357 (2000).
[36] X.-M. Qian, T. Zhang, C. Chang *et al.*, Rev. Sci. Instrum. **74**, 4096 (2003).
[37] K. Müller-Dethlefs and E. W. Schlag, Annu. Rev. Phys. Chem. **42**, 109 (1991).
[38] C. Y. Ng, Annu. Rev. Phys. Chem. **53**, 101 (2002).
[39] P. M. Johnson, in *Photoionization and Photodetachment*, edited by C. Y. Ng (World Scientific, Singapore, 2000), p. 296.
[40] M. Evans, S. Stimson, C. Y. Ng, C.-W. Hsu, and G. K. Jarvis, J. Chem. Phys. **110**, 315 (1999).
[41] C.-W. Hsu, M. Evans, C. Y. Ng, and P. Heimann, Rev. Sci. Instrum. **68**, 1694 (1997).
[42] C.-W. Hsu, P. Heimann, M. Evans, S. Stimson, P. T. Fenn, and C. Y. Ng, J. Chem. Phys. **106**, 8931 (1997).
[43] G. K. Jarvis, Y. Song, and C. Y. Ng, Rev. Sci. Instrum. **70**, 2615 (1999).
[44] P. A. Heimann, M. Koike, C. W. Hsu *et al.*, Rev. Sci. Instrum. **68**, 1945 (1997).
[45] G. K. Jarvis, K.-M. Weitzel, M. Malow, T. Baer, Y. Song, and C. Y. Ng, Rev. Sci. Instrum. **70**, 3892 (1999).
[46] X. Qian, T. Zhang, C. Chang *et al.*, Rev. Sci. Instrum. **74**, 4096 (2003).
[47] X. Qian, T. Zhang, Y. Chiu, D. J. Levandier, J. S. Miller, R. A. Dressler, and C. Y. Ng, J. Chem. Phys. **118**, 2455 (2003).
[48] T. Zhang, X. M. Qian, X. N. Tang, C. Y. Ng, Y. Chiu, D. J. Levandier, J. S. Miller, and R. A. Dressler, J. Chem. Phys. **119**, 10175 (2003).
[49] X. N. Tang, H. Xu, T. Zhang, Y. Hou, C. Chang, C. Y. Ng, Y. Chiu, R. A. Dressler, and D. J. Levandier, J. Chem. Phys. **122**, 164301 (2005).
[50] V. Aquilanti, G. Capecchi, S. Cavalli, D. D. Fazio, P. Palmieri, C. Puzzarini, A. Aguilar, X. Gimenez, and J. M. Lucas, Chem. Phys. Lett. **318**, 619 (2000).
[51] P. Palmieri, C. Puzzarini, V. Aquilanti, G. Capecchi, S. Cavalli, D. D. Fazio, A. Aguilar, X. Gimenez, and J. M. Lucas, Mol. Phys. **98**, 1839 (2000).
[52] P. Pendergast, J. M. Heck, E. F. Hayes, and R. Jaquet, J. Chem. Phys. **98**, 4543 (1993).
[53] N. E. Bradbury and R. A. Nielsen, Phys. Rev. **49**, 388 (1936).
[54] P. R. Vlasak, D. J. Beussman, M. R. Davenport, and C. G. Enke, Rev. Sci. Instrum. **67**, 68 (1996).
[55] K. Norwood and C. Y. Ng, Chem. Phys. Lett. **156**, 145 (1989).
[56] C. Y. Ng, in *Vacuum Ultraviolet Photoionization and Photodissociation of Molecules and Clusters*, edited by C. Y. Ng (World Scientific, Singapore, 1991), p. 169.
[57] S. Stimson, Ph.D. thesis, Iowa State University, 1998.
[58] S. Stimson, Y.-J. Chen, M. Evans, C.-L. Liao, C. Y. Ng, C.-W. Hsu, and P. Heimann, Chem. Phys. Lett. **289**, 507 (1998).
[59] A. Henglein, in *Ion-Molecule Reactions in the Gas Phase*, edited by P. J. Ausloos (American Chemical Society, Washington, DC, 1966), Vol. 58, p. 63.
[60] A. Henglein and K. Lacmann, Adv. Mass Spectrom. **3**, 331 (1966).
[61] M. Sizun and F. Aguillon, Chem. Phys. **226**, 47 (1998).
[62] M. Sizun, F. Aguillon, V. Sidis, V. Zenevich, G. D. Billing, and N. Markovic, Chem. Phys. **209**, 327 (1996).

[63] Z. Herman and I. Koyano, J. Chem. Soc., Faraday Trans. 2 **83**, 127 (1987).
[64] P. J. Kuntz and A. C. Roach, J. Chem. Soc., Faraday Trans. 2 **68**, 259 (1972).
[65] E. F. Hayes, A. K. Q. Siu, J. F. M. Chapman, and R. L. Matcha, J. Chem. Phys. **65**, 1901 (1976).
[66] C. Stroud and L. M. Raff, Chem. Phys. **46**, 313 (1980).
[67] J. Urban, R. Jaquet, and V. Staemmler, Int. J. Quantum Chem. **38**, 339 (1990).
[68] J. Urban, V. Klimo, V. Staemmler, and R. Jaquet, Z. Phys. D: At., Mol. Clusters **21**, 329 (1991).
[69] J. D. Kress, R. B. Walker, and E. F. Hayes, J. Chem. Phys. **93**, 8085 (1990).
[70] M. Gilibert, X. Giménez, F. Huarte-Larrañaga, M. González, A. Aguilar, I. Last, and M. Baer, J. Chem. Phys. **110**, 6278 (1999).
[71] F. Huarte-Larrañaga, X. Giménez, J. M. Lucas, A. Aguilar, and J. M. Launay, Phys. Chem. Chem. Phys. **1**, 1125 (1999).
[72] F. Huarte-Larrañaga, X. Giménez, J. M. Lucas, A. Aguilar, and J. M. Launay, J. Phys. Chem. **104**, 10227 (2000).
[73] P. M. Dehmer and W. A. Chupka, J. Chem. Phys. **65**, 2243 (1976).
[74] M. A. O'Halloran, P. M. Dehmer, F. S. Tomkins, S. T. Pratt, and J. L. Dehmer, J. Chem. Phys. **89**, 75 (1988).
[75] D. Gerlich (private communication).
[76] R. D. Levine and R. B. Bernstein, J. Chem. Phys. **56**, 2281 (1972).
[77] C. Rebick and R. D. Levine, J. Chem. Phys. **58**, 3942 (1973).
[78] G. Gioumousis and D. P. Stevenson, J. Chem. Phys. **29**, 294 (1958).
[79] R. M. Bilotta and J. M. Farrar, J. Chem. Phys. **75**, 1776 (1981).
[80] M. Sizun and E. A. Gislason, J. Chem. Phys. **91**, 4603 (1989).
[81] X. N. Tang, H. F. Xu, C. Houchins, K.-C. Lau, Y. Chiu, D. J. Levandier, R. A. Dressler, and C. Y. Ng (unpublished).
[82] S. Civis, J. Sebera, V. Spirko, J. Fiser, W. P. Kraemer, and K. Kawaguchi, J. Mol. Struct. **695–696**, 5 (2004).
[83] N. Sathyamurthy, Chem. Phys. Lett. **59**, 95 (1978).
[84] N. Sathyamurthy, Chem. Phys. **62**, 1 (1981).
[85] N. Sathyamurthy, R. Rangarajan, and L. M. Raff, J. Chem. Phys. **64**, 4606 (1976).
[86] P. J. Kuntz and W. N. Whitton, Chem. Phys. Lett. **34**, 340 (1975).
[87] W. N. Whitton and P. J. Kuntz, J. Chem. Phys. **64**, 3624 (1976).
[88] N. Sathyamurthy and L. M. Raff, J. Chem. Phys. **63**, 464 (1975).
[89] C. Zuhrt, F. Schneider, U. Havemann, L. Zülicke, and Z. Herman, Chem. Phys. **38**, 205 (1979).
[90] T. Joseph and N. Sathyamurthy, J. Chem. Phys. **80**, 5332 (1984).
[91] T. Joseph and N. Sathyamurthy, J. Chem. Phys. **86**, 704 (1987).
[92] S. Kumar, H. Kapoor, and N. Sathyamurthy, Chem. Phys. Lett. **289**, 361 (1998).
[93] J. T. Adams, Chem. Phys. Lett. **33**, 275 (1975).
[94] N. Balakrishnan and N. Sathyamurthy, Comput. Phys. Commun. **63**, 209 (1991).
[95] D. J. Kouri and M. Baer, Chem. Phys. Lett. **24**, 37 (1974).
[96] N. Balakrishnan and N. Sathyamurthy, Chem. Phys. Lett. **201**, 294 (1993).
[97] N. Balakrishnan and N. Sathyamurthy, Chem. Phys. Lett. **240**, 119 (1995).
[98] T. Joseph and N. Sathyamurthy, J. Indian Chem. Soc. **62**, 874 (1985).
[99] S. Mahapatra and N. Sathyamurthy, J. Chem. Phys. **102**, 6057 (1995).
[100] S. Mahapatra and N. Sathyamurthy, J. Chem. Phys. **105**, 10934 (1996).
[101] K. Sakimoto and K. Onda, Chem. Phys. Lett. **226**, 227 (1994).
[102] N. Sathyamurthy, M. Baer, and T. Joseph, Chem. Phys. **114**, 73 (1987).
[103] C. Kalyanaraman, D. C. Clary, and N. Sathyamurthy, J. Chem. Phys. **111**, 10910 (1999).
[104] S. Mahapatra and N. Sathyamurthy, J. Chem. Phys. **107**, 6621 (1997).
[105] B. Maiti, S. Mahapatra, and N. Sathyamurthy, J. Chem. Phys. **113**, 59 (2000).
[106] J. Z. H. Zhang, D. L. Yeager, and W. H. Miller, Chem. Phys. Lett. **173**, 489 (1990).
[107] B. Lepetit and J. M. Launay, J. Chem. Phys. **95**, 5159 (1991).
[108] B. Maiti, C. Kalyanaraman, A. Panda, and N. Sathyamurthy, J. Chem. Phys. **117**, 9719 (2002).
[109] A. K. Tiwari, A. N. Panda, and N. Sathyamurthy, J. Phys. Chem. A **110**, 389 (2006).
[110] T.-S. Chu, R.-F. Lu, and K.-L. Han, X.-N. Tang, H.-F. Xu, and C. Y. Ng, J. Chem. Phys. **122**, 244322 (2005).
[111] A. N. Panda and N. Sathyamurthy, J. Chem. Phys. **122**, 054304 (2005).
[112] J. A. Coxon and P. G. Hajigeorgiou, J. Mol. Spectrosc. **193**, 306 (1999).
[113] P. J. Chantry, J. Chem. Phys. **55**, 2746 (1971).
[114] D. Gerlich, R. Disch, and S. Scherbarth, J. Chem. Phys. **87**, 350 (1987).
[115] L. S. Sunderlin and P. B. Armentrout, Chem. Phys. Lett. **167**, 188 (1990).
[116] P. Tosi, F. Boldo, F. Eccher, M. Filippi, and D. Bassi, Chem. Phys. Lett. **164**, 471 (1989).
[117] P. Tosi, O. Dmitriev, and D. Bassi, Chem. Phys. **97**, 3333 (1992).
[118] P. Tosi, G. Fontana, S. Longano, and D. Bassi, Int. J. Mass Spectrom. Ion Process. **93**, 95 (1989).
[119] Y. Song, M. Evans, C. Y. Ng, C.-W. Hsu, and G. K. Jarvis, J. Chem. Phys. **111**, 1905 (1999).
[120] Y. Song, M. Evans, C. Y. Ng, C.-W. Hsu, and G. K. Jarvis, J. Chem. Phys. **112**, 1306 (2000).
[121] G. K. Jarvis, M. Evans, C. Y. Ng, and K. Mitsuke, J. Chem. Phys. **111**, 3058 (1999).
[122] G. K. Jarvis, Y. Song, and C. Y. Ng, J. Chem. Phys. **111**, 1937 (1999).
[123] M. Evans and C. Y. Ng, J. Chem. Phys. **111**, 8879 (1999).
[124] J. Hepburn, J. Chem. Phys. **107**, 7106 (1997).
[125] Y. Morioka, Y. Lu, T. Matsui, T. Tanaka, H. Yoshii, T. Hayaishi, and R. I. Hall, J. Chem. Phys. **104**, 9375 (1996).
[126] S. R. Mackenzie and T. P. Softley, J. Chem. Phys. **101**, 10609 (1994).
[127] R. J. Green, J. Qian, H.-T. Kim, and S. L. Anderson, J. Chem. Phys. **113**, 3002 (2000).
[128] A. H. Kung and Y. T. Lee, in *Vacuum Ultraviolet Photoionization and Photodissociation of Molecules and Clusters*, edited by C. Y. Ng (World Scientific, Singapore, 1991), p. 487.
[129] J. W. Hepburn, in *Vacuum Ultraviolet Photoionization and Photodissociation of Molecules and Clusters*, edited by C. Y. Ng (World Scientific, Singapore, 1991), p. 435.
[130] U. Hollenstein, H. Palm, and F. Merkt, Rev. Sci. Instrum. **71**, 4023 (2000).
[131] C. Chang, Y. Hou, C. Houchins, M.-K. Bahng, and C. Y. Ng (unpublished).
[132] L. Y. Baranov, A. Held, H. L. Selzle, and E. W. Schlag, Chem. Phys. Lett. **291**, 311 (1998).
[133] A. Held, L. Y. Baranov, H. L. Selzle, and E. W. Schlag, Chem. Phys. Lett. **291**, 318 (1998).
[134] S. Hannemann, U. Hollenstein, E.-J. van Duijn, and W. Ubachs, Opt. Lett. **30**, 1494 (2005).
[135] S. T. Park, H. L. Kim, and M. S. Kim, Bull. Korean Chem. Soc. **23**, 1247 (2002).
[136] S. T. Park, S. Y. Kim, and M. S. Kim, J. Chem. Phys. **114**, 5568 (2001); **115**, 2492 (2001).
[137] C. Chang, Y. Hou, C. Houchins, C. Y. Ng, and R. A. Dressler (unpublished).
[138] P. Wang, X. Xing, K.-C. Lau, H. K. Woo, and C. Y. Ng, J. Chem. Phys. **121**, 7049 (2004).
[139] X. Zhang, A. V. Friderichsen, J. T. McKinnon, T. G. Lindeman, D. E. David, D. C. Dayton, S. Nandi, G. B. Ellison, and M. R. Nimlos, Rev. Sci. Instrum. **74**, 3077 (2003).
[140] S. Nourbakhsh, K. Norwood, G.-Z. He, and C. Y. Ng, J. Am. Chem. Soc. **113**, 6311 (1991).
[141] *Imaging in Chemical Dynamics*, edited by A. G. Suits and R. E. Continetti (American Chemical Society, Washington, DC, 2001), Vol. 770.
[142] E. L. Reichert, G. Thurau, and J. C. Weisshaar, J. Chem. Phys. **117**, 653 (2002).
[143] E. L. Reichert and J. C. Weisshaar, J. Phys. Chem. A **106**, 5563 (2002).